Article ID: 1000-7032(2025)07-1326-07

Synthesis, Mechanical Characteristic and Near-infrared Reflective Property of Perylene Diimide-containing Polyurethane

SONG Yifan[1,2], LI Zixin[1], TIAN Kaili[1*], BERMESHEV Maxim V[3], HU Yanghao[1], SU Yupeng[2], WANG Jie[2], PAN Hongfei[2], LI He[2], REN Xiangkui[1,2*]

(1. *Tianjin Key Laboratory of Membrane Science and Desalination Technology, School of Chemical Engineering and Technology, Tianjin University, Tianjin* 300350, *China*;
2. *Zhejiang Institute of Tianjin University, Ningbo* 315201, *China*;
3. *A. V. Topchiev Institute of Petrochemical Synthesis of Russian Academy of Sciences, Moscow* 119991, *Russia*)
* *Corresponding Authors, E-mail: tkl*168@*tju. edu. cn*; *renxiangkui@tju. edu. cn*

Abstract: Doping perylene diimide(PDI) into a polymer matrix is a simple strategy to prepare near-infrared(NIR) reflective materials, but the mechanical properties and NIR reflectance properties are significantly compromised due to macro-phase separation. In this study, a novel polymer(denoted as PU-PDI) with intrinsic NIR reflective properties was synthesized by covalent incorporation of PDI units into polyurethane chains. Its photophysical characteristics, mechanical property and NIR reflectance property are investigated in detail. The results show that covalent incorporation reduces the severe aggregation of PDI units, thereby endows PU-PDI with excellent mechanical property. The elongation at break of PU-PDI can reach more than 700%, and the breaking strength is 34. 11 MPa. Moreover, compared to the blending system, PU-PDI possesses enhanced NIR reflection ability due to the better dispersion of PDI units.

Key words: perylene diimide; polyurethane; near-infrared(NIR) reflectance
CLC number: O482. 31 **Document code**: A
DOI: 10. 37188/CJL. 20250043 **CSTR**: 32170. 14. CJL. 20250043

含苝酰亚胺聚氨酯的合成、力学特性及近红外反射性能

宋一凡[1,2], 李子欣[1], 田凯丽[1*], BERMESHEV Maxim V[3], 胡杨浩[1], 苏玉鹏[2], 王 婕[2], 潘宏斐[2], 李 赫[2], 任相魁[1,2*]

(1. 天津大学 化工学院, 天津市膜科学与海水淡化技术重点实验室, 天津 300350;
2. 天津大学浙江研究院, 浙江 宁波 315201;
3. 俄罗斯科学院 A.V. Topchiev 石化合成研究所, 俄罗斯 莫斯科 119991)

摘要: 在聚合物基体中掺杂苝酰亚胺(PDI)是制备近红外(NIR)反射材料的常用方法,但PDI与聚合物的宏观相分离通常会严重影响材料的力学性能和近红外反射性能。本研究通过共价键将PDI分子引入到聚氨酯高分子链,合成了一种具有本征近红外反射性能的新型聚合物PU-PDI,并对其光物理特性、力学性能和近红外反射性能开展了详细研究。结果表明,共价接入的方法可有效抑制PDI单元的聚集,使PU-PDI具有优异的

收稿日期: 2025-02-26; **修订日期**: 2025-03-07
基金项目: 国家自然科学基金(22175129,22475149); 宁波市“科创甬江2035”重点研发计划国际科技合作项目(2024H017)
Supported by National Natural Science Foundation of China (22175129, 22475149); the International Sci-tech Cooperation Project Under the “Innovation Yongjiang 2035” Key R&D Programme (2024H017)

力学性能。PU-PDI的断裂伸长率可达700%以上,断裂强度为34.11 MPa。此外,与共混体系相比,由于PDI具有更好的分散性,PU-PDI具有更优异的近红外反射性能。

关　键　词: 苝酰亚胺; 聚氨酯; 近红外(NIR)反射

1　Introduction

Near-infrared (NIR) radiation (700−2 500 nm) constitutes 52% of solar radiation[1-2]. However, most materials are unable to effectively reflect the radiation in the NIR region. This leads to an increase in the internal energy of materials and environmental heat accumulation, accelerating material loss and increasing energy consumption for processes such as refrigeration[3-4]. Therefore, the development of materials with high NIR reflectivity has become a research hotspot. In recent years, the NIR reflective pigments reported in the literature are mainly concentrated in inorganic pigments and metal oxide pigments, such as titanium dioxide, zincoxide and chromium oxide[5-7]. However, with the development of green chemistry[8], low-toxicity, low-cost and high-performance organic pigments have gradually become the focus of attention.

Perylene diimide (PDI) derivatives exhibit excellent chemical stability, high colorability and optical properties[9-10], making them widely employed in high-performance dyes, photoelectric devices[11], luminous solar concentrators[12] and other fields. Research has shown that some PDI derivatives have high transparency in the NIR region, providing great potential for the development of NIR reflective materials[13-14]. However, the large conjugated plane and rigid structure of PDI molecules promote strong π-π stacking, which adversely affects their optical properties and processability[15-17]. In order to address this issue, PDI units were induced into the polymer matrix to regulate the intermolecular interaction, thereby optimizing material properties. The incorporation of PDI molecules and polymer not only guarantees photoactive molecules have sufficient dispersion space[18-19], but also provides excellent stability and mechanical properties, bringing remarkable advantages for the practical application[20].

Currently, introducing PDI into polymer system *via* physical blending has emerged as a highly promising strategy for developing high-performance NIR reflective films. The physical blending method is relatively easy to operate and cost-effective, which is beneficial for industrial production and large-scale application[21-22]. However, the implementation of this strategy still encounters a series of challenges. Among them, achieving uniform dispersion of PDI in the polymer matrix is a primary issue[23-24]. The aggregation of PDI molecules not only diminishes its reflection capabilities but may also cause internal stress concentration in the material, adversely affecting the overall film performance[25-26]. Furthermore, the processing stability of the system cannot be overlooked. During the polymer processing, factors such as high temperature and shear forces can result in PDI degradation or migration, thereby compromising the NIR reflective properties and long-term stability of the material[27-28]. Therefore, although introducing PDI into the polymer system through physical blending shows great potential in enhancing the performance of NIR reflective films, the issues of uniform dispersion of PDI, processing stability of the system, and balanced optimization of comprehensive performance remain critical scientific challenges in the research of PDI-based NIR reflective films[28].

In this study, a novel polymer (denoted as PU-PDI) with NIR reflective property was synthesized by bonding the PDI chromophores to the polyurethane (PU) matrix covalently. Experiments demonstrate that the covalent bond between the PDI segments and the polyurethane chains ensures better dispersion of PDI within the polymer matrix. As a result, compared with the physically blended system PU/PDI, PU-PDI possesses enhanced tensile property and NIR reflection ability in the range of 700 nm to 2 500 nm.

2 Experiment

2.1 Materials

1, 6, 7, 12-Tetrachloro-3, 4, 9, 10-tetracarboxylic dianhydride, 1-aminooctane, 6-amino-1-hexanol, 2-n-octyl-1-dodecylamine, poly(tetrahydrofuran)(PTMG, M_n=1 000 g/mol), polycaprolactone diol(PCDL, M_n=2 000 g/mol) and terephthalohydrazide(TD, 95%) were purchased from Tianjin Xi'ensiaopude Technology Co., Ltd. Isophorone diisocyanate(IPDI, 99%) was purchased from Shanghai Aladdin Biochemical Technology Co., Ltd. Dibutyltin dilaurate (DBTDL, 98%), N, N-Dimethylformamide(DMF, 99.9%, molecular sieves), methylene chloride(DCM), methanol(MeOH), petroleum ether(PE) and toluene were purchased from Anhui Zesheng Technology Co., Ltd. And were used without further purification unless otherwise specified.

2.2 Synthesis and Characterizations

The synthetic route of PDI, PU-PDI and PU/PDI is illustrated in Fig. 1. Detailed procedures and characterization data are provided in the Supplementary Information. The PDI content in PU-PDI and PU/PDI is the same, and the mass fraction is 1%.

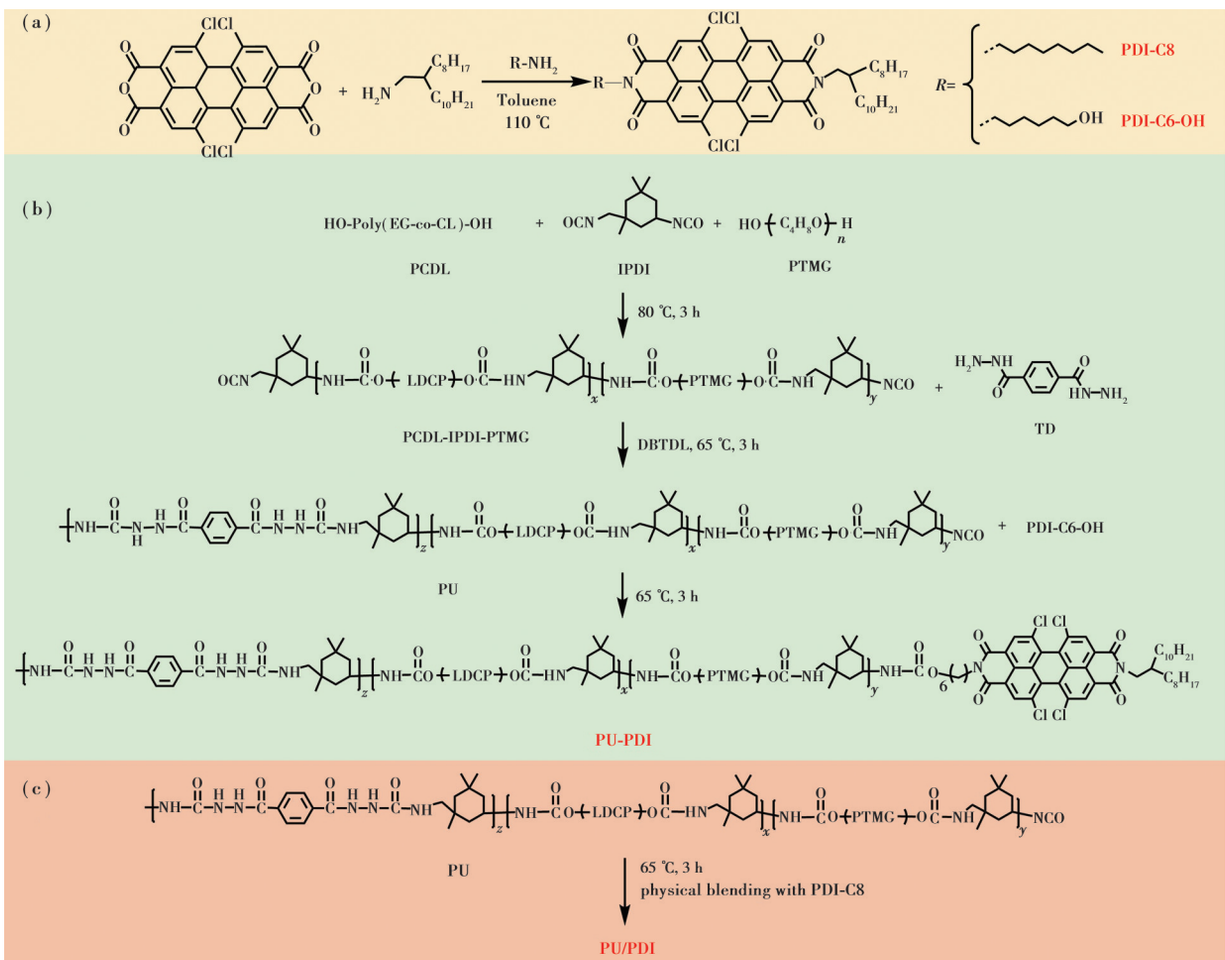

Fig.1 Synthesis process of PDI(a), PU-PDI(b) and PU/PDI(c)

3 Results and Discussion

3.1 FT-IR Spectra Analysis of PU-PDI

The structure of the final compound PU-PDI was confirmed by FT-IR spectra(Fig. 2) and ^{1}H NMR (Fig. S1). As shown in Fig. 2, there is no N═C═O tensile vibration peak corresponding to IPDI monomer near 2 250–2 275 cm^{-1}. The tensile vibration peaks corresponding to N—H and C═O of the carbamate bond appear at 3 325 cm^{-1}. The disappearance of isocyanate bond and the appearance of carbamate bond proved the successful synthesis of PU-PDI. The antisymmetric stretching vibration peaks corresponding to methylene appear at 2 939 cm^{-1} and 2 859 cm^{-1},

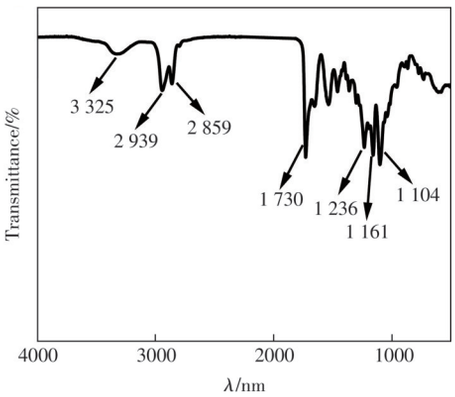

Fig.2　The FT-IR of PU-PDI

and the stretching vibration peaks of ether bonds appear at 1 104 cm^{-1}. The stretching vibration peaks corresponding to ester group C—O appear at 1 161 cm^{-1} and 1 236 cm^{-1}, which proves that PCDL has been successfully introduced into PU-PDI.

3.2　Photophysical Properties and Aggregation Structure

To investigate the optical properties and aggregation behavior of PU-PDI and PU/PDI, UV-Vis absorption and photoluminescence spectra were measured. As shown in Fig. 3, the absorption peaks of PU-PDI and PU/PDI at 520 nm, 486 nm and 426 nm correspond to the vibrational structures of PDI chromophores, which are attributed to the S_{0-0}, S_{0-1}, and S_{0-2} vibronic transitions, respectively. Notably, the absorption ratio of the S_{0-0} to S_{0-1} transitions in PU/PDI is reduced, indicating that the PU/PDI forms more pronounced aggregation through stronger π-π stacking interactions. Furthermore, compared to that of PU-PDI, the photoluminescence spectrum of PU/PDI reveals a pronounced bathochromic shift, further confirming the presence of PDI aggregation.

To further investigate the aggregation behavior of the samples, X-ray diffraction (XRD) measurements were conducted. As shown in Fig. 4, PU/PDI exhibits strong diffraction peaks, suggesting a certain degree of aggregation and crystallinity of PDI molecules and poor compatibility of PDI-C8 within the PU matrix. In contrast, no obvious diffraction peaks can be observed for PU-PDI, indicating the homogeneous distribution of PDI segments in the polymer matrix. Furthermore, the SEM images of PU-PDI

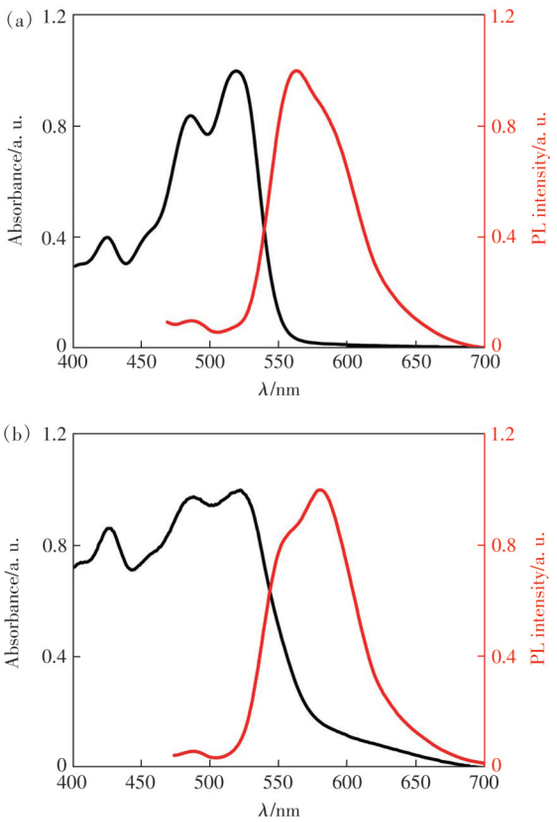

Fig.3　UV-Vis absorption spectra (black line) and photoluminescence spectra (red line) of PU-PDI(a) and PU/PDI(b)

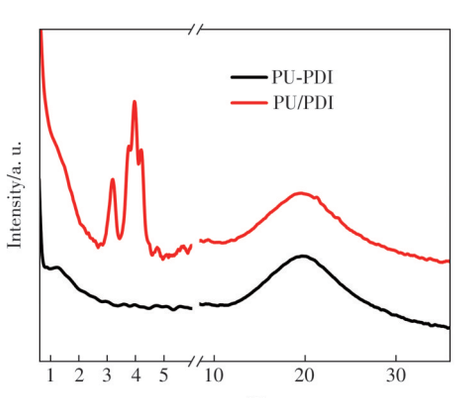

Fig. 4　XRD patterns of PU-PDI and PU/PDI

and PU/PDI(Fig. 5) showed that the surface of PU-PDI was relatively smooth, while the surface of PU/PDI was rough with a large number of massive aggregates, which is in accordance with XRD results.

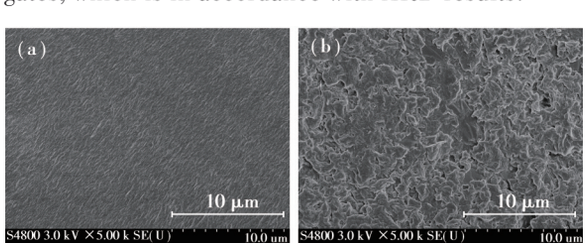

Fig.5　SEM images of PU-PDI(a) and PU/PDI(b)

3.3 Thermal Stability and Mechanical Properties

The TGA and DMA curves of PU, PU-PDI and PU/PDI are displayed in Fig. 6 and Fig. S2, respectively. Fig. 6 indicates that the thermal decomposition degrees of these materials are very close, and the corresponding decomposition temperature is about 280 ℃. Fig. S2 shows that the glass transition temperatures of PU, PU-PDI and PU/PDI are −30.74 ℃, −30.74 ℃, −32.63 ℃, respectively. The result indicates that the introduction of PDI has no obvious impact on the thermal stability of polyurethane materials, and the good thermal stability of polyurethane materials can be retained.

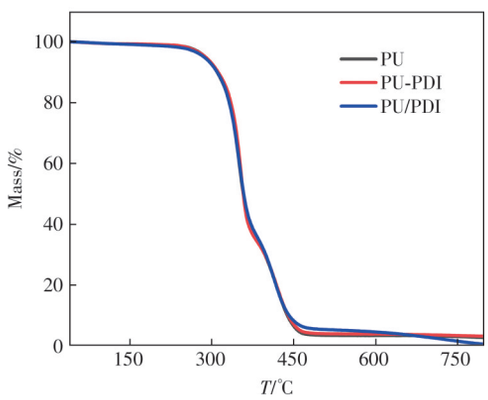

Fig.6 TGA curves of PU, PU-PDI and PU/PDI

To determine how the two incorporation approaches affect the mechanical properties, the stress-strain tests of PU, PU/PDI and PU-PDI were conducted. As shown in Fig. 7, compared to pristine PU, PU/PDI shows a significant decrease in both tensile strength and elongation at break, likely due to the excessive aggregation of PDI molecules within the PU matrix, leading to material defects and severely compromising the mechanical properties.

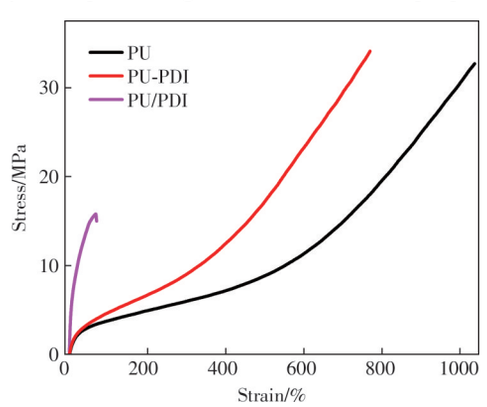

Fig.7 Stress-strain curves of PU, PU-PDI and PU/PDI

However, PU-PDI exhibits a slight increase in breaking strength and a slight reduction in elongation at break, indicating the retaining of PU's comprehensive mechanical property. As shown in Fig. S2, the energy storage modulus of the three materials exhibits minimal difference, but the tanδ of PU-PDI is stably higher than that of PU, indicating that PU-PDI possesses better damping performance.

3.4 NIR Reflective Properties

In order to study the NIR reflective properties of PU-PDI and PU/PDI, the UV-Vis-NIR reflectance spectra were obtained by UV-Vis-NIR spectrophotometry on white substrate. As shown in Fig. 8, PU-PDI and PU/PDI indicate obvious absorption in visible region due to the nature of PDI chromophore. However, both PU-PDI and PU/PD show high reflectance in NIR region. In particular, the reflectance values progressively increased in the 700−1 750 nm wavelength interval. This region (700−1 750 nm) accounts for higher than 80% of the NIR solar energy, and so it has important effect on cool activity of the pigments. In detail, PU-PD exhibits better NIR reflectance, which should be related to the homogeneous distribution of PDI chromophores within the polymer matrix through chemical grafting. The good dispersibility results in a more homogeneous molecular network, preventing the light scattering of PDI aggregations. In contrast, PU/PD shows a relatively lower NIR reflectance due to the significant aggregation of PDI molecules, which disrupts the homogenization of the material and increases light scattering and absorption. As shown in Tab. 1, the average NIR reflectance of PU-PDI was higher than that of

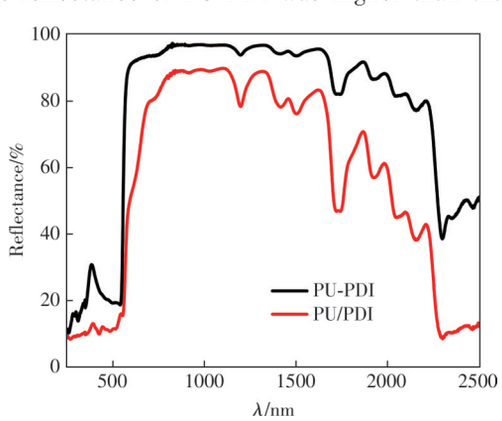

Fig.8 UV-Vis-NIR reflectance spectra of PU-PDI and PU/PDI

Tab. 1　Average NIR reflectance values

Samples	700−1 750 nm	1 750−2 500 nm	700−2 500 nm
PU-PDI	95%	72%	85%
PU/PDI	82%	39%	61%

PU/PDI, and the NIR reflectance value of PU-PDI can reach to 95%.

4　Conclusion

In summary, we designed and synthesized a PDI-based polyurethane(PU-PDI) by covalent incorporation strategy. The UV-Vis absorption spectra, photoluminescence spectra and XRD results indicate that, compared to the physically blended system PU/PDI, the PDI units exhibit good dispersion within the PU matrix. The stress-strain curve result shows that the elongation at break of PU-PDI exceeds 700% and the tensile strength is 34.11 MPa, indicating PU-PDI retains the good mechanical properties of PU. The UV-Vis-NIR reflectance spectra demonstrate that PU-PDI has excellent NIR reflectance. Overall, these results provide a feasible design strategy for the fabrication of PDI-based polyurethane films with NIR reflective properties.

Supplementary Information and Response Letter are available for this paper at: http://cjl.lightpublishing.cn/thesisDetails#10.37188/CJL.20250043

References:

[1] MAZHAR M, ABDOUSS M, ZARIFI F, *et al*. Effectiveness of perylene pigment on the reduction of energy demand of a building [J]. *Pigm. Resin Technol.*, 2020, 49(4): 265-271.

[2] COZZA E S, ALLOISIO M, COMITE A, *et al*. NIR-reflecting properties of new paints for energy-efficient buildings [J]. *Sol. Energy*, 2015, 116: 108-116.

[3] LIBBRA A, TAROZZI L, MUSCIO A, *et al*. Spectral response data for development of cool coloured tile coverings [J]. *Opt. Laser Technol.*, 2011, 43(2): 394-400.

[4] GRAMM G, FUHRMANN G, ZIMMERHOFER F, *et al*. Development of high NIR-reflective red Li_2MnO_3 pigments [J]. *Z. Anorg. Allg. Chem.*, 2020, 646(21): 1722-1729.

[5] IRENI N G, KARUPPAIAH M, NARAYAN R, *et al*. TiO_2/poly(thiourethane-urethane)-urea nanocomposites: anticorrosion materials with NIR-reflectivity and high refractive index [J]. *Polymer*, 2017, 119: 142-151.

[6] 傅竹西, 林碧霞, 何一平, 等. ZnO薄膜的反射、透射光谱及能带结构测量 [J]. 发光学报, 2002, 23(6): 559-562.
FU Z X, LIN B X, HE Y P, *et al*. Reflection and transmission spectra of ZnO films and its band-gap structure [J]. *Chin. J. Lumin.*, 2002, 23(6): 559-562. (in Chinese)

[7] LI Y Q, MEI S G, BYON Y J, *et al*. Highly solar radiation reflective Cr_2O_3-$3TiO_2$ orange nanopigment prepared by a polymer-pyrolysis method [J]. *ACS Sustain. Chem. Eng.*, 2014, 2(2): 318-321.

[8] ANASTAS P, EGHBALI N. Green chemistry: principles and practice [J]. *Chem. Soc. Rev.*, 2010, 39(1): 301-312.

[9] 张丹, 刘婕, 石栋, 等. 基于硅氧烷修饰的苝二酰亚胺氟离子荧光传感器 [J]. 发光学报, 2021, 42(6): 855-862.
ZHANG D, LIU J, SHI D, *et al*. Fluorescent sensor for fluoride ions based on perylene diimide tethered with siloxane moieties [J]. *Chin. J. Lumin.*, 2021, 42(6): 855-862. (in English)

[10] 顾丹丹, 赵浩儒, 江晓泽, 等. 羧基改性苝酰亚胺与钙离子的络合组装及荧光增强 [J]. 发光学报, 2025, 46(3): 474-485.
GU D D, ZHAO H R, JIANG X Z, *et al*. Complexation and fluorescence enhancement of bay-site carboxyl modified perylene dimide with calcium ion [J]. *Chin. J. Lumin.*, 2025, 46(3): 474-485. (in English)

[11] 李志成, 妙亚, 刘少伟, 等. PTCDI-C8作为阴极修饰层提高钙钛矿太阳能电池的性能 [J]. 发光学报, 2018, 39(9): 1291-1296.
LI Z C, MIAO Y, LIU S W, *et al*. Performance improvement of planar heterojunction perovskite solar cells by using PTCDI-C8 as cathode buffer layer [J]. *Chin. J. Lumin.*, 2018, 39(9): 1291-1296. (in English)

[12] LI Y L, OLSEN J, NUNEZ-ORTEGA K, *et al*. A structurally modified perylene dye for efficient luminescent solar concentrators [J]. *Sol. Energy*, 2016, 136: 668-674.

[13] KAUR B, BHATTACHARYA S N, HENRY D J. Interpreting the near-infrared reflectance of a series of perylene pigments [J]. *Dyes Pigm.*, 2013, 99(2): 502-511.

[14] MARTINI F, MINEI P, LESSI M, *et al*. Structural order and NIR reflective properties of perylene bisimide pigments: experimental evidences from a combined multi-technique study [J]. *Dyes Pigm.*, 2020, 179: 108401.

[15] WÜRTHNER F, THALACKER C, SAUTTER A, *et al*. Hierarchical self-organization of perylene bisimide-melamine assemblies to fluorescent mesoscopic superstructures [J]. *Chem. Eur. J.*, 2000, 6(21): 3871-3886.

[16] YANG L, YU Y Y, ZHANG J, *et al*. Time-dependent aggregation-induced enhanced emission, absorption spectral broadening, and aggregation morphology of a novel perylene derivative with a large D-π-a structure [J]. *Chem. Asian J.*, 2015, 10(5): 1215-1224.

[17] WÜRTHNER F, THALACKER C, DIELE S, *et al*. Fluorescent *J*-type aggregates and thermotropic columnar mesophases of perylene bisimide dyes [J]. *Chem. Eur. J.*, 2001, 7(10): 2245-2253.

[18] HU D F, PENG L Y, XU W J, *et al*. Ultrathin near-infrared transmitting films enabled by deprotonation-induced intramolecular charge transfer of a dopant [J]. *Nat. Commun.*, 2024, 15(1): 8197.

[19] ZHANG X Y, TIAN K L, LIU J, *et al*. Perylene diimide Incorporated polyurethane polymer as potential colour filter material with non-fluorescent property [J]. *Chin. J. Chem.*, 2023, 41(11): 1348-1354.

[20] TIAN K L, HUANG H J, BERMESHEV M V, *et al*. Perylene diimide tethered with multi-POSS nanocages for polymer composite material with nonlinear optical property [J]. *Dyes Pigm.*, 2024, 229: 112270.

[21] CONTINI E, DINI V A, ROZZI A, *et al*. Comparative mechanochromic performance of perylene diimide-doped polyurethanes: blending *vs* bonding [J]. *ACS Appl. Polym. Mater.*, 2024, 6(1): 669-680.

[22] LING Z C, ZHOU Q X. Effects of NIR-reflective pigments on waterborne polyurethane coatings and their thermal insulation performance [J]. *Prog. Org. Coat.*, 2024, 196: 108678.

[23] MAZHAR M, ABDOUSS M, GHARANJIG K, *et al*. Synthesis, characterization and near infra-red properties of perylenebisimide derivatives [J]. *Prog. Org. Coat.*, 2016, 101: 297-304.

[24] MAHMOUDI MEYMAND F, MAZHAR M, ABDOUSS M. Investigation of substituent effect on cool activity of perylene bisimide pigments [J]. *J. Coat. Technol. Res.*, 2019, 16(2): 439-447.

[25] LIU J, GAO S Y, ZHANG X K, *et al*. POSS-containing polynorbornene with pendant perylene diimide: from a unique supramolecular structure to tunable luminescence properties [J]. *J. Mater. Chem.* C, 2022, 10(22): 8791-8796.

[26] 李子欣, 黄汉军, YOU SOMARY, 等. 自愈合发光聚氨酯弹性体的制备与性能 [J]. 发光学报, 2023, 44(6): 985-994.
LI Z X, HUANG H J, YOU S, *et al*. Preparation and properties of self-healing luminescent polyurethane elastomer [J]. *Chin. J. Lumin.*, 2023, 44(6): 985-994. (in Chinese)

[27] WANG M, ZHANG Q J, LI Z, *et al*. Solvents effects on film morphologies and memory behavior of a perylenediimide-containing pendent polymer [J]. *Chem. Asian J.*, 2018, 13(14): 1784-1790.

[28] MINEI P, LESSI M, CONTIERO L, *et al*. Boosting the NIR reflective properties of perylene organic coatings with thermoplastic hollow microspheres: optical and structural properties by a multi-technique approach [J]. *Sol. Energy*, 2020, 198: 689-695.

宋一凡(2000-),女,山东济宁人,硕士研究生,2022年于济南大学获得学士学位,主要从事聚氨酯材料及苝酰亚胺小分子研究。
E-mail: songyifan@tju.edu.cn

任相魁(1980-),男,河北邢台人,博士,教授,2010年于南开大学获得博士学位,主要从事小分子及高分子材料的聚集态结构及性能研究。
Email: renxiangkui@tju.edu.cn

田凯丽(1999-),女,河北保定人,博士研究生,2021年于河北大学获得学士学位,主要从事苝酰亚胺衍生物的制备及性能研究。
Email: tkl168@tju.edu.cn